Title:

Serine chirality guides metabolic flow between one-carbon metabolism and neuromodulator synthesis

Masataka Suzuki[1,2,12#], Kenichiro Adachi[1#], Pattama Wiriyasermukul[3,4], Mariko Fukumura[5], Ryota Tamura[5], Yoshinori Hirano[9], Yumi Aizawa[6], Tetsuya Miyamoto[7], Sakiko Taniguchi[1], Masahiro Toda[5], Hiroshi Homma[7], Kohsuke Kanekura[8], Kenji Yasuoka[9], Takanori Kanai[10], Masahiro Sugimoto[6], Shushi Nagamori[3], Masato Yasui[1], and Jumpei Sasabe[1.10,11.12]

1. Department of Pharmacology, Keio University School of Medicine, 35 Shinanomachi, Shinjuku-ku, Tokyo 160-8582, Japan.
2. Current address; Division of Infectious Diseases, Brigham and Women's Hospital, Boston, MA, USA.
3. Center for SI Medical Research and Department of Laboratory Medicine, The Jikei University School of Medicine, Tokyo, 105-8461, Japan.
4. Current address; Department of Biological Chemistry, Faculty of Agriculture, Iwate University, Iwate, 020-8550, Japan
5. Department of Neurosurgery, Keio University School of Medicine, 35 Shinanomachi, Shinjuku-ku, Tokyo 160-8582, Japan.
6. Institute of Medical Science, Tokyo Medical University, Shinjuku, Tokyo, Japan
Institute for Advanced Biosciences, Keio University, Tsuruoka, Yamagata, Japan
7. Graduate School of Pharmaceutical Sciences, Kitasato University, 5-9-1 Shirokane, Minato-ku, Tokyo 108–8641, Japan
8. Department of Pharmacology, Tokyo Medical University, 6-1-1 Shinjuku, Shinjuku-ku, Tokyo 160-8402, Japan.
9. Department of Mechanical Engineering, Keio University, 3-14-1 Hiyoshi, Kohoku-ku, Yokohama, Kanagawa 223-8522, Japan
Laboratory for Computational Molecular Design, RIKEN Center for Biosystems Dynamics Research (BDR), Suita, Osaka 565-0874, Japan
10. Department of Internal Medicine, Keio University School of Medicine, 35 Shinanomachi, Shinjuku-ku, Tokyo 160-8582, Japan.
11. Human Biology-Microbiome-Quantum Research Center (WPI-Bio2Q), Keio University, Tokyo 160-8582, Japan
# These authors contributed equally.

12 To whom correspondence should be addressed: Masataka Suzuki and Jumpei Sasabe
Department of Pharmacology, Keio University School of Medicine, 35 Shinanomachi, Shinjuku-ku, Tokyo 160-8582 Japan. Phone: +81-3-5363-3750. Fax: +81-3-3359-8889. E-mail: masataka.s@keio.jp; sasabe@keio.jp

Abstract (150 words)
Neural development requires metabolic adaptations that coincide with a functional shift from differentiation to neurotransmission. Serine metabolism provides essential metabolites for cellular growth and proliferation, and also produces neurotransmitters. However, how serine metabolism coordinates functional development of neurons remains unclear. Here, we report that neurons undergo metabolic transitions through an enantiomeric shift of serine during functional maturation. Developmental alterations of neural transcriptional profiles and serine enantiomers indicated that L- to D-serine conversion is a signature of neural maturation. Metabolomic analysis of neural progenitors revealed that D-serine decreases glycine synthesis, thereby suppressing one-carbon metabolism, in which L-serine is a crucial carbon donor. D-serine inhibits one-carbon metabolism by competing with transport of cytosolic L-serine to mitochondria, which restrains proliferation and triggers apoptosis of neural progenitors as well as neural tumor cells, but not mature neurons, *in vitro* and *ex vivo*. Thus, our findings suggest that the metabolic transition from L- to D-serine during neural maturation inhibits one-carbon metabolism essential for proliferation of immature neural cells, leading to acquisition of characteristics tailored to functional development toward neurotransmission. (174)

Introduction

Serine is a unique amino acid, both L- and D-enantiomers of which are synthesized *de novo* in the central nervous system. L-serine is primarily synthesized from a glycolytic intermediate through the phosphorylated pathway, and further stereo-converted to D-serine (Fig. 1a). Serine enantiomers and their metabolites are critically involved in neural development and neurophysiology in three major ways. First, L-serine is a crucial carbon donor with the cofactor, folate for the one-carbon metabolism, which is a universal metabolic process for nucleic acid synthesis, methylation, and reductive metabolism. As these pathways essentially support proliferative cells, undifferentiated or cancer cells are particularly susceptible to deprivation of L-serine or inhibition of *de novo* L-serine synthesis(*1*). Second, biosynthesis of membrane lipids requires L-serine as an integral component of sphingolipids and phosphatidylserine. The nervous system includes highly polarized neurons and glia, and has the highest lipid content/complexity in the mammalian body. Among membrane lipids, sphingolipids are particularly abundant in the nervous system and are essential for neuronal differentiation, polarization, synapse formation, and myelination, which are required for development and functional integrity of the nervous system(*2*). Third, L-serine serves as a precursor for neurotransmitters, such as glycine and D-serine. L-serine is converted to glycine by serine hydroxymethyltransferase (Shmt) in the one-carbon metabolic pathway, and also into D-serine by serine racemase (Srr). Both glycine and D-serine bind physiologically, albeit with different affinities, to the obligatory (GluN1) and regulatory (GluN3) subunits of *N*-methyl-D-aspartate (NMDA) receptors, which regulate excitatory neurotransmission and are crucial in development and functions of the central nervous system(*3*, *4*). In addition, glycine also binds to inhibitory glycine receptors and controls early embryonic development as well as a variety of motor and sensory functions(*5*).

Defects of L-serine synthesis due to single nucleotide polymorphisms in the genes encoding 3-phosphoglycerate dehydrogenase (PHGDH), the rate-limiting enzyme in the phosphorylated pathway, or the downstream enzyme phosphoserine aminotransferase (PSAT1) are associated with congenital microcephaly and hypomyelination, and exhibit psychomotor retardation and seizures in humans (*6*, *7*). Phgdh deficient mice die in embryo after 13.5 days post-coitum and show systemic growth defects, especially severe hypoplasia of the central nervous system, with marked reductions of L-serine and sphingolipids(*8*). Indeed, proliferative-marker-positive cells and mature neurons are almost entirely absent in these mice, indicating that *de novo* biosynthesis of L-serine is critical for neural proliferation and differentiation. Given that L-serine synthesis impacts diverse metabolites in one-carbon metabolism, lipid synthesis, and neurotransmitters glycine and D-serine(*9*), L-serine likely serves multiple functions in neural development. Of note, serine synthesis shows drastic changes after neurogenesis. Neural progenitor cells (NPCs) express PHGDH, whereas mature neurons lack its expression and lose the ability to synthesize L-serine. In mature neural tissue, on the other hand, astrocytes take over L-serine synthesis, and supply neurons with L-serine for synthesis of neurotransmitter D-serine. Despite the fact that neural tissue undergoes such dynamic shifts in serine metabolism after development, it still remains unclear how serine metabolism is involved in functional changes during neural development.

In this study, we sought to understand transitions of serine-associated metabolism during neural development and to clarify how serine enantiomers are involved in functional changes with neural differentiation. Our results reveal that D-serine is a hallmark of mature neurons and that it suppresses one-carbon metabolism by competing with L-serine transport to mitochondria in immature cells.

Main

Enantiomeric shift of serine metabolism during neural development

Serine metabolism is fundamental to multiple cellular functions (Fig. 1a) and crucial for neural development. Neurophysiological significance of serine metabolism should change along with development of cellular functions, but its developmental changes have not been comprehensively understood. To understand developmental alteration of serine metabolism in the central nervous system, we first monitored serine enantiomers and glycine using a two-dimensional HPLC system (2D HPLC), a highly sensitive tool to quantify amino acid enantiomers. L-serine levels in the mouse cerebral cortex showed a gradual increase during embryonic development, dropped at birth, and remained at a concentration above 500 nmol/g thereafter (Fig. 1b). As glycine synthesis depends in part on L-serine, glycine showed a similar trend to L-serine in embryo and maintained levels above 800 nmol/g after birth (Fig.1b). On the other hand, D-serine, a coagonist of NMDA receptors(*10*, *11*), was trace during the embryonic stage, but increased gradually after birth. Therefore, the D/L-serine ratio exhibited a steady increase after birth and reached 0.4 in mature mouse brain (Fig. 1b). The dynamics of serine enantiomers during the brain development is corroborated by transcriptional profiles associated with serine metabolism. Bulk RNA-seq data of developing neurons derived from mouse embryonic stem cells (ESC)(*12*) or human inducible pluripotent stem cells (iPSC)(*13*) in public databases showed that diverse transcriptions found in the phosphorylated pathway of L-serine synthesis (PHGDH, PSAT1, and PSPH), one-carbon metabolism (SHMT1/2, MTHFD1/2, and MTHFD1/2L), and nucleic acid synthetic pathway (DHFR, TYMS, MTHFS) decrease along with the neuronal differentiation (Fig. S1a, b). In contrast, D-serine-synthetic enzyme SRR increases after days *in vitro* 7 (DIV7) in ESC-derived neurons and NPC/Rosetta cells (DIV14-21) in human iPSC-derived neurons. Subunits of NMDA receptors, including Grin1/GluN1, to which D-serine or glycine binds, are expressed in matured neurons after DIV16 of mouse ESC-derived cells (Fig. S1a) or those at DIV49 of human iPSC-derived cells (Fig. S1b). Alterations of serine metabolism during development were further supported by single-cell RNA-seq performed by Di Bella et al.(*14*), which provides crucial information about the trajectory of differentiating cells and cell type-specific transcriptional profiles during mouse brain development *in vivo*. Uniform manifold approximation and projection (UMAP) illustrates that Sox2+ neural progenitor cells (cluster 1, 7, 9, and 11) express L-serine synthetic enzymes (Phgdh, Psat1, Psph) and folate cycle enzymes (Tyms, Mthfd1, Dhfr) as well as a proliferation marker gene Mki67 (Fig. 1c, Fig. S1c, d). Apoe+ and Aldh1l1+ astrocytes (cluster 7) also express L-serine synthetic pathways, whereas Tubb3+ mature neurons (cluster 0, 2, 3, 4, 5, 8, 12, 13, 15, 16, 19, 22) do not express serine synthetic enzymes (Fig.1c, Fig.S1c, d). Tubb3+ neurons weakly express Srr at P4 but not E10 (Fig. S1e). These transcriptional profiles suggest that reduction of L-serine biosynthesis during neural development accompanies inactivation of the folate cycle and one-carbon metabolism, and that mature neurons start to synthesize D-serine. Given that the folate cycle and one-carbon metabolism, essential for nucleic acid biosynthesis, are the metabolic signature of cell proliferation, NPCs lose their metabolic activity for proliferation in the embryonic stage but instead develop the capacity for neurotransmission during the postnatal development.

D-serine inhibits cell proliferation and induces apoptosis

D-serine is a characteristic metabolite of mature neurons (Fig. 1b, c). Although the functional role of D-serine as a neurotransmitter has been well characterized, its metabolic significance during development is not well understood. To test whether D-serine affects neural development, we made a primary culture of NPCs from telencephalon in E14 mice in serine-free Neurobasal medium, treated with D- or L-serine from DIV1. At DIV7, L-serine treatment significantly increased the number of neurons with a condensed neurites compared to vehicle-treated neurons. In contrast, D-serine-treated culture had fewer number of neurons with sparse neurites, suggesting that D-serine hindered differentiation of NPCs (Fig. 1d, e). Furthermore, D-serine activated cleavage of caspase-3 dose-dependently in Nestin-positive NPCs and Tubb3+ developing neurons 48 h after treatment, whereas L-serine had no effect (Fig. 1f-i, Fig. S2a-c). In contrast, vesicular glutamate transporter 2 (vGlut2)-positive mature excitatory neurons, glutamate decarboxylase-67 (Gad67)-positive mature inhibitory neurons, and glial fibrillary acidic protein (Gfap)-positive glial cells did not

undergo apoptosis under D- or L-serine treatment (Fig. 1h and i, Fig. S2d and e). Susceptibility of NPCs was pronounced in the presence of D-serine, but was not caused by other D-amino acids, such as D-aspartate, D-alanine, or D-proline (Fig. S3a), which can also be detected in mammalian intestinal bacteria(*15*). Therefore, while degradation of diverse D-amino acids by mammalian oxidases yields cytotoxic hydrogen peroxide(*16*), D-serine-specific toxicity did not support involvement of oxidases for D-amino acids in cell death induced by D-serine. We further tested whether D-serine neurotoxicity involves NMDA receptors(*17*). Blockade of Ca^{2+} influx through NMDA receptors by a non-competitive NMDA antagonist, MK-801, or of D-serine-binding to the receptors by 5,7-dichlorokynurenic acid (DCKA) did not attenuate D-serine neurotoxicity (Fig. S3b and c). Also, inhibition of the receptor's downstream signal by *N*-nitro-L-arginine methylester (L-NAME) or an anti-oxidant (glutathione) did not affect enhanced cleavage of caspase-3 by D-serine (Fig. S3d and e). Thus, our findings suggest that apoptosis triggered by D-serine in NPCs mediates a previously unrecognized pathway.

D-serine restrains L-serine/glycine one-carbon metabolism

To test whether apoptosis triggered by D-serine involves amino acid metabolism, we supplemented NPCs treated with D-serine from DIV1 with various L-amino acids or glycine. Notably, among L-amino acids and glycine, L-serine specifically and dose-dependently inhibited cleavage of caspase-3 caused by D-serine (Fig. 2a and b). Since D- and L-enantiomers have the same chemical composition, we hypothesized that D-serine competes with L-serine metabolism. During the neuronal development, NPCs require L-serine for synthesis of two distinct membrane sphingolipids and phospholipids, to expand their cell bodies and to elongate their axons and dendrites. Synthesis of sphingolipids and phospholipids from L-serine mediates two pathways (Fig. S4a). A comparative lipidomic study using NPCs revealed that D-serine treatment increased phosphatidylserine, but not sphingolipids or other phospholipids (Fig. S4b, c). To further study whether D-serine is incorporated into phosphatidylserine, we extracted membrane lipids, removed serine from phosphatidylserine using phospholipase D (PLD), and quantified serine enantiomers using 2D HPLC (Fig. S4d, e). Phosphatidylserine extracted from NPCs cultured without D-serine harbored only L-serine, but supplementation with D-serine significantly increased phosphatidyl-D-serine and decreased phosphatidyl-L-serine (Fig. S4f). Addition of L-serine to D-serine-treated NPCs completely inhibited this increase of phosphatidyl-D-serine (Fig. S4f). However, supplementation with phosphatidyl-L-serine itself did not rescue NPCs from D-serine-induced apoptosis (Fig. S4g), indicating that loss of phosphatidyl-L-serine in membrane lipids appears not to trigger apoptosis.

To understand whether L-serine impacts other metabolic pathways, we compared metabolomic profiles in NPCs treated with or without serine enantiomers. As D-serine induces apoptosis and L-serine rescues NPCs from it, we searched for the metabolites that change in parallel with the effects of serine enantiomers. Among detected metabolites, glycine was significantly reduced by D-serine and recovered by supplementation with L-serine (Fig. 2c and Fig. S5a, b), which was also quantitatively confirmed using 2D HPLC (Fig. 2de). Pathway analysis using our metabolomic findings indicated that glycine, serine, and threonine metabolism was significantly affected by D-serine treatment (Fig. S5c). Indeed, in the central nervous system, glycine is synthesized from L-serine by serine hydroxymethyltransferase (Shmt) 1 and 2 (Fig. 2f), which performs the first transfer of a carbon unit from L-serine to folate in one-carbon metabolism, an essential process for nucleotide synthesis(*18*). Since ES-derived cultured neurons and iPSC-derived neurons express one-carbon enzymes, such as Shmt1/2, during development (Fig. 2f and Fig. S1a, b), we hypothesized that D-serine may inhibit the initial step, which transfers a carbon unit from L-serine thereby suppressing one-carbon metabolism. As expected, D-serine treatment of NPCs reduced production of formate, an intermediate of the folate cycle in one-carbon metabolism, whereas L-serine enhanced it (Fig. 2g). Furthermore, supplementation of NPCs with an upstream intermediate, 5,10-methylenetetrahydrofolate (5,10-meTHF), attenuated cleavage of caspase-3 triggered by D-serine (Fig. 2h). Given that one-carbon metabolism is crucial for cell proliferation and survival, these findings support our view that D-serine slows cell proliferation and triggers apoptosis by restricting one-carbon metabolism.

D-serine suppresses one-carbon metabolism by competing with L-serine transport to mitochondria

In the presence of mitochondrial Shmt2, transfer of a carbon unit from L-serine to tetrahydrofolate (THF) and glycine production depends primarily on mitochondrial enzyme, but not cytoplasmic Shmt1 (Fig. 3a)(*19*). Since immature neurons express Shmt2 (Fig. 2f and Fig. S1a-c), the mitochondrial one-carbon pathway is crucial for cell proliferation and survival. Therefore, the molecular target of D-serine in its inhibition of the initial step of one-carbon metabolism is likely mitochondrial Shmt2 or supply of its substrates into mitochondria (Fig. 3a). To study whether D-serine impacts catalytic activity of Shmt2, we compared homotetrameric assembly of human SHMT2 combined with either L- or D-serine in the presence of THF and pyridoxal phosphate (PLP) (Fig. S6). When L- or D-serine was placed in the binding pocket of Shmt2, the eliminating carbon in D-serine was more distant from phosphorus (P) and oxygen (O) in PLP by 1.50 Å (C-P) and 1.10 Å (C-O) than that in L-serine (Fig. 3b and Fig. S6a and b), suggesting that D-serine is not a good substrate for SHMT2. To investigate the stability of serine enantiomers in the binding pocket, we further performed molecular dynamic (MD) simulation of the serine-bound SHMT2 complex systems. MD simulation indicated that binding of D-serine did not affect the overall structure of SHMT2 compared to that of L-serine (Fig. S6c). On the other hand, molecular interactions of D-serine with SHMT2 were unstable and D-serine could not stay in the serine-binding pocket of SHMT2, which is supported by a recent report that SHMT does not use D-serine as a substrate in the canonical hydroxymethyl-transferase reaction in one-carbon metabolism(*20*). In contrast, L-serine remained placed stably in the pocket (Fig. 3c and Supplementary movie1). Therefore, D-serine was unlikely to compete with L-serine binding to SHMT2. Indeed, an *in vitro* experiment using recombinant SHMT2 showed that D-serine did not affect conversion of L-serine to glycine (Fig. 3d).

Next, we wondered whether D-serine inhibits supply of Shmt2 substrate(s), L-serine or THF, to mitochondria. Since reduction of glycine caused by D-serine in NPCs was compensated by addition of L-serine, but not of THF (Fig. 2d, 3e), we assumed that L-serine supply to mitochondria is disturbed by D-serine. Moreover, in NPCs, endogenous L-serine synthesis was not disturbed by addition of D-serine (Fig. 2e), suggesting that D-serine affect L-serine transport to mitochondria, but not its synthesis. To confirm that D-serine impacts L-serine transport to mitochondria, we semi-permeabilized a neuroblastoma cell line, Neuro2a, to loosen cell membranes and monitored [H^3]L-serine transport into mitochondria and other organelles in the presence or absence of D-serine. Intriguingly, D-serine competitively inhibited transport of L-serine in a dose-dependent manner (IC50, 1.604 mM) (Fig. 3f). Competitive transport of serine enantiomers to mitochondria and other organelles was consistent with dose-dependent rescue of D-serine-induced apoptosis by L-serine (Fig. 2b). Thus, these results suggested that D-serine impairs one-carbon metabolism by competing with L-serine transport to mitochondria, but not by direct inhibition of Shmt2 activity.

To further understand the overall response of immature neurons to the D-serine insult, we performed RNA-sequencing using Neuro2a cells treated with D-serine. D-serine mildly, but significantly altered the transcriptome profile compared with vehicle control (Fig. 3g,h). There were 685 up-regulated genes ($\log_2$ fold-change > 0, adjusted p-value < 0.05) and 905 down-regulated genes ($\log_2$-fold change < 0, adjusted p-value < 0.05) (Fig. 3h). To determine whether genes with significant alterations are clustered in specific functional gene sets, we performed gene set enrichment analysis. Notably, D-serine enhanced expressions of genes associated with mitochondrial functions, such as respiratory chain complex assembly, ATP synthesis driven by proton motive force, and mitochondrial gene expression / translation. On the other hand, gene sets linked to amino acid import across the plasma membrane, cellular growth, and neuron projection extension were down-regulated (Fig.3ij, Fig.S7). These dynamic transcriptional changes support our findings that D-serine inhibits polarization and growth/proliferation of immature neurons (Fig. 1d,e), and further indicate that immature neurons resist D-serine-induced cellular stress by enhancing mitochondrial function, including energy synthesis.

D-serine inhibits tumor cell growth

Brain tumor cells with high proliferative capacity share characteristics with neural stem cells(*21*). Given that D-serine inhibits proliferation and induces apoptosis in NPCs through inhibition of one-carbon metabolism (Fig. 1-3), we wondered whether brain tumor cells might have similar metabolic

vulnerabilities(*1*, *22–24*). To test this idea, we treated several human/rodent neuroblastoma cell lines cultured in the regular medium containing sub-millimolar L-serine and fetal bovine serum with D-serine. Consistent with our findings that D-serine inhibits cell proliferation by competing with L-serine transport (Fig. 3f), high concentrations of D-serine were required to decrease the viability of neuroblastoma cell lines cultured in regular medium (Fig. S8a). In contrast, culturing in L-serine/glycine-free medium with dialyzed fetal bovine serum reduced the viability of Neuro2a cells with much lower D-serine concentrations (IC50 = 1.94 mM) (Fig. S8b-d), which corresponds to the efficacy of D-serine on inhibition of L-serine transport (IC50 = 1.604 mM) (Fig. 3f). Indeed, with L-serine/glycine-free medium, D-serine significantly decreased viabilities of all neuroblastoma cell lines tested, at low millimolar concentrations (Fig. 4a). In accordance with its effect on NPCs, D-serine inhibited production of glycine and reduced viability of Neuro2a cells, which was rescued by supplementation with L-serine (Fig. 4b and Fig. S8e). Moreover, supplementations with glycine and downstream metabolites of the folate cycle in the one-carbon pathway (Fig. 2f), such as formate, inosine monophosphate (IMP), or 5,10-meTHF, phenocopied the rescue effect by L-serine (Fig. S8e-i). On the other hand, combinations of glycine and metabolites of the methionine cycle (methionine or methylcobalamin (meCbl)) as well as other metabolites associated with one-carbon metabolism (thymidine monophosphate (dTMP) or glutathione) (Fig. 2f) failed to liberate cells (Fig. S8j, k). These results suggest that D-serine impacts the folate cycle rather than the methionine cycle in one-carbon metabolism to prevent growth of neuroblastoma cells in a manner similar to that of NPCs.

As NPCs give rise to neuronal as well as glial cell types, we further tested whether glial tumor cells also show vulnerability to D-serine. Glioblastoma is the most common malignant brain tumor in adults, whose survival rate is low despite advances in surgical and medical neuro-oncology(*23*, *24*). Among human glioblastoma cell lines (U87, U251, SF126), U251 cells were the most vulnerable to D-serine treatment (Fig.4c). Supplementation with glycine and formate restored viability of U251 (Fig. 4d), and 5,10-meTHF recovered the vulnerability to D-serine, albeit very mildly (Fig, 4e), supporting the significance of one-carbon metabolism in growth of glioblastoma cell lines. To further test the anti-proliferative effect of D-serine in the tumor microenvironment, we made an organotypic brain slice culture from mice with orthotopic xenografts of glioblastoma cells expressing Venus fluorescence(*25*). Brain slices of mice implanted with U87 cells in the striatum were cultured *ex vivo* for 7 days in serine/glycine-free media containing D-serine or vehicle. D-serine strikingly suppressed expansion of U87 cells with Venus fluorescence compared to the control treatment, even in *ex vivo* tumor culture (Fig. 4f, g). Since glioma stem cells (GSCs) in the glioblastoma have self-renewal and tumor-initiating capacity and cause cancer recurrence(*26*, *27*), we wondered whether GSCs also have similar vulnerability to D-serine. *In vitro*, D-serine reduced viability of cell lines for GSCs (hG008 and hG020), established from human glioblastoma specimens[25], in a dose-dependent manner with greater efficacy to the hG008 line (Fig. 4h). This growth defect in hG008 cells induced by D-serine was rescued by supplementation with glycine and formate, as in neuroblastoma and glioblastoma cells (Fig. S8l). hG008 cells have a sphere-forming capacity[23], and we also observed D-serine-induced reduction of sphere diameters of hG008 cells cultured under the sphere-forming conditions (Fig. 4i). Moreover, in brain slices of mice with orthotopic xenografts of hG008 cells expressing Venus fluorescence, D-serine significantly inhibited growth and invasiveness of hG008 cells (Fig. 4j, k). Thus, in a manner similar to NPCs, brain tumors showed consistent vulnerability to D-serine via inhibition of one-carbon metabolism.

Discussion

We found that D-serine, synthesized by neurons as a sign of maturation, inhibits cell proliferation in immature neural cells. NPCs synthesize and metabolize L-serine for proliferation and differentiation, and upon maturation as neurons, switch their metabolism to specialize in L- to D-serine stereo-conversion. While D-serine functions in the extracellular space as a neurotransmitter in mature neurons, it competes intracellularly with mitochondrial L-serine transport, which inhibits further proliferation by inactivating one-carbon metabolism. Consistent with dependence of proliferation on one-carbon metabolism, various immature cells, including cancer cells, are sensitive to the inhibitory effect of D-serine on one-carbon metabolism. Thus, neurons switch synthesis of serine enantiomers to effect a functional shift from proliferation to neurotransmission.

In the central nervous system, L-serine increases during fetal development and declines rapidly after birth, while D-serine increases only after birth and reaches the mature levels within a few weeks (Fig. 1). This postnatal increase of D-serine is consistent with a previous report in rats(*28*) and can be explained by a gradual increase of Srr after birth in mouse glutamatergic neurons (Fig. S1a and e) or forebrain tissue(*29*). In the mature brain, the majority of Srr is restricted to neurons(*29*, *30*), which coincides with our view that D-serine synthesis is a sign of neuronal maturation. In contrast, PHGDH is not expressed in neurons, but is confined to astrocytes in mature brain(*9*). This astrocyte-specific expression of the L-serine synthetic enzyme accords with our findings that a set of genes encoding enzymes for L-serine synthesis and one-carbon metabolism are downregulated in mature neurons, but confined to a cell population with mature astrocyte markers (Fig. 1c and S1). Given that astrocytes require one-carbon metabolism for proliferation and that neurons prioritize neurotransmission, such cell-type specific and enantio-selective serine metabolism in the matured brain appears to be a reasonable metabolic compartmentalization. Indeed, loss of D-serine synthesis does not trigger developmental abnormalities(*29*), but causes functional or structural abnormalities in mature neurons(*31–34*). Furthermore, supplementation with D-serine in the neonatal brain enhances functional development of forebrain neurons(*35*). Therefore, it is likely that D-serine does not promote differentiation of NPCs, but contributes to functional maturation of differentiated neurons.

While D-serine is important for functional maturation of neurons as well as excitatory neurotransmission through NMDA receptors(*10*, *31*, *33*), D-serine has an inhibitory effect on proliferation and triggers apoptosis in NPCs and other immature cells (Fig. 1 and 4). Extracellular D-serine is a classic trigger of excitotoxicity in neurons(*36*, *37*), whereas it induces intracellularly necrosis/apoptosis in renal tubular cells at high doses(*38*, *39*). Excitotoxicity of D-serine has been reported in mature neurons in ischemic or neurodegenerative diseases and mediates NMDA receptors (*36*, *40–42*). In contrast, the D-serine toxicity, which we observed in neural culture, occurs only in immature neurons, and can be rescued by L-serine or intermediates of the one-carbon metabolism, but not by inhibitors of NMDA receptors or their downstream signals (Fig. 1fhi and 2agh and S3). The latter toxicity reported in kidneys mediates hydrogen peroxide generated through degradation of D-serine by a D-serine catabolic enzyme, D-amino acid oxidase, plentiful in kidneys(*43*). Nonetheless, D-amino acid oxidase is not expressed in neurons or in the forebrain(*44*). Furthermore, as we could not find protective effects by an antioxidant against D-serine toxicity in immature neurons (Fig. S3e), involvement of oxidative stress by hydrogen peroxide is unlikely. Thus, D-serine toxicity observed in this study does not appear mediated by mechanisms previously reported. Importantly, a recent report suggests that renal tubular toxicity by D-serine can be ameliorated by L-serine(*45*). Although the authors did not demonstrate involvement of one-carbon metabolism in D-serine toxicity in the kidneys, their observation could be associated with our findings that D-serine functionally competes with L-serine (Fig. 2ab).

We show that D-serine attenuates cell proliferation by inhibiting one-carbon metabolism (Fig. 3). Since proliferative cells require one-carbon units for nucleotide synthesis and methylation (Fig. 2f), one-carbon metabolism is crucial for both developmental and proliferative tissues(*46*). As we observe that immature cells are susceptible to D-serine (Fig. 1hi), demand for one-carbon units is highest in fetal development(*46*). Indeed, in humans, deficiency of L-serine or folate, which receives one-carbon units from L-serine, leads to congenital defects in the central nervous system(*47*, *48*). Supply of one-carbon units from L-serine has both

cytoplasmic and mitochondrial branches in one-carbon metabolism (Fig. 2f), but the mitochondrial pathway is critical in embryonic development(*46*, *49*). Therefore, transport of L-serine, generated in the cytoplasm, into mitochondria appears to be a critical step for cellular proliferation during development. A seminal study by Kory et al. has shown that sideroflexin 1, a multipass inner mitochondrial membrane protein, and its homologs mediate L-serine transport to mitochondria(*50*). Notably, they show *in vitro* that D-serine competes with L-serine transport through sideroflexin 1. Together with our results from an *in vivo* L-serine competition assay (Fig. 3f), D-serine may compete with general L-serine transport to mitochondria through transporters, such as sideroflexin homologs. In addition, *de novo* serine synthesis and mitochondrial one-carbon pathway are required for the proliferative phenotype in a large variety of human cancers(*51–55*). Therefore, the broad anti-proliferative effect of D-serine on neural tumor cells (Fig. 4) supports our idea that D-serine inhibits the mitochondrial one-carbon pathway. Since cancer genetics indicate two pathways not targeted by existing therapies, de novo serine synthesis and mitochondrial one-carbon metabolism(*46*, *56*), inhibition of L-serine transport to mitochondria, such as by potent D-serine derivatives, to disconnect these two pathways might be a reasonable target for development of cancer therapeutants.

Neuronal metabolism exhibits the unique property of serine isomerization to adapt to functional maturation (Fig. 1). Consequently, mature cerebrum contains sub-millimolar levels of D-serine, which account for a quarter of total serine in the cerebrum and are about 100-times higher than blood levels(*57*). This active stereo-conversion of serine in the cerebrum is unique to mammals among vertebrates(*58*), implying that neurophysiological functions of D-serine are inseparable from the functional evolution of the cerebrum in higher vertebrates. Indeed, whereas either D-serine or glycine are required to activate NMDA receptors, D-serine binds to the GluN1 subunit of NMDA receptors with higher affinity than does glycine(*59*) and also has an inhibitory effect on the GluN3 subunit by competing with glycine(*4*). Therefore, extracellular D-serine appears to be evolutionarily important as a neurotransmitter, with different properties than glycine. On the other hand, the inhibitory function of intracellular D-serine against mitochondrial one-carbon metabolism (Fig. 2 and 3) may be an evolutionarily inherited trait from the biological ancestors of mitochondria, bacteria(*60*). Notably, bacteria depend on one-carbon metabolism for their growth, and D-serine attenuates bacterial growth by inhibiting L-serine metabolism(*61*). Therefore, bacterial sensitivity to D-serine may reveal a common pathway for inhibition of mitochondrial one-carbon metabolism by D-serine. Given that neurons do not express enzymes for mitochondrial one-carbon metabolism upon maturation (Fig. S1), evolutionary acquisition of neurophysiological functions of D-serine without cytotoxicity may be due to the fact that mature neurons are not proliferative and do not depend on this conserved metabolic feature of mitochondria. While complete understanding of the significance of serine stereo-conversion in the developmental brain will require further studies to illuminate neurogenesis under spatio-temporally controlled D-serine, this study provides a basis to understand the significance of developmental dynamics of serine enantiomer synthesis.

Materials and Methods

Animals

All animal experiments were approved by the institutional Animal Experiment Committee and conducted in accordance with Institutional Guidelines on Animal Experimentation at Keio University. C57BL/6Jjcl mice were purchased from CLEA Japan (Tokyo, Japan). ICR mice were from Charles River Laboratories (Wilmington, MA, USA). Female BALB/c nude mice (BALB/cSlc-nu/nu) were from Japan SLC (Shizuoka, Japan). Mice were raised in 12 h light and dark cycle with free access to food (CE-2, CLEA Japan) and water in the specific pathogen-free environment.

Antibodies

Rabbit polyclonal antibodies to cleaved caspase-3 and to GAPDH were purchased from Cell Signaling Technologies (Danvers, MA, USA). Mouse monoclonal antibodies to GFAP, vGLUT2, and GAD67 were from Agilent Technologies (Santa Clara, CA, USA), Abcam (Cambridge, UK), and Merck Millipore (Darmstadt, Germany), respectively.

Cell culture and viability assay

NPCs and primary cultured astrocytes (PCAs) were prepared as follows. Telencephalon tissues from ICR mice were dissected at the embryonic day 14, treated with papain, and disassembled by pipetting. The cell suspension was passed through a 40-μm filter, centrifuged, and resuspended in a Neurobasal medium without serine (NB-S) (Research Institute for the Functional Peptide, Yamagata, Japan). NPCs were cultured in NB-S supplemented with 2% B-27 supplement (ThermoFisher, Waltham, MA, USA), 1% Penicillin-streptomycin solution (ThermoFisher), and 1% GlutaMAX supplement (ThermoFisher). For PCAs, NPCs were differentiated into astrocytes within 7 days by changing the medium to D-MEM (high glucose) (Fujifilm Wako, Tokyo, Japan) supplemented with 10% FBS (A5256701, ThermoFisher) and 1% Penicillin-Streptomycin at 24 h *in vitro*.

Neuroblastoma (Neuro2a, F11, NSC34, and SHSY5Y) and glioma (U87, U251, SF126) cell lines were cultured in MEM supplemented with 10% dialyzed FBS (S-FBS-NL-065, SERENA Europe GmbH, Brandenburg, Germany), 5 mM D-glucose, 65 μM sodium pyruvate, 1 × MEM vitamin solution (ThermoFisher), 2 mM L-glutamine, 0.15 mM L-proline, 0.15 mM L-alanine, 0.15 mM L-aspartic acid, 0.15 mM L-glutamic acid, and 0.34 mM L-asparagine (-SG media) as described in Tajan et al.(*62*), unless otherwise noted. Viability of NPCs, PCAs, and cancer cell lines was analyzed with Cell Counting Kit-8 in accordance with the manufacture's protocol (Dojindo, Kumamoto, Japan).

Western blot

NPCs were harvested in a lysis buffer [50 mM Tris-HCl, pH 7.4, 150 mM NaCl, 20 mM ethylenediaminetetraacetate (EDTA), 1% TritonX-100, protease inhibitor cocktail (Sigma-Aldrich, St. Louis, MO, USA)]. Protein concentration was analyzed with a BCA assay kit (ThermoFisher), and 20-80 μg of protein were subjected to SDS-PAGE. Then, proteins were transferred to the PVDF membranes and blocked with 10% skim milk in PBST. Proteins were detected with anti-cleaved caspase-3 antibody or ant-GAPDH antibody (Cell Signaling Technology, MA, USA), and HRP-conjugated secondary antibodies (Jackson ImmunoResearch Laboratories, PA, USA).

Metabolomics

Cells were washed twice with 10 mL of PBS(-). The PBS(-) was aspirated, and 1 mL of MeOH containing internal standards was added to the dish. The dish was left for 10 min, and a sample solution was obtained and transferred to a tube. For metabolite extraction, the tube was vortexed and subsequently centrifuged at 20,380×g for 10 minutes at 4 °C (MDX-310, TOMY Seiko, Tokyo, Japan). The 150 μL of supernatant was transferred to another tube and dried by centrifugation at 1,600 rpm (366×g) for 90 min at room temperature (VC-96W, Taitec, Saitama, Japan). Then, 10 μL of 90% MeOH were added, 30 μL of

H_2O were added and mixed, and then the tube was centrifuged at 20,380×g for 10 minutes at 4 °C. The 20 μL of supernatant were transferred to a vial and injected into the LC-MS system.

The LC-MS instrument has previously been described in detail(*63*). Briefly, an Agilent Technologies 1290 Infinity LC system and a G6230B time-of-flight MS (TOF–MS) (Agilent Technologies, Santa Clara, CA, USA) were used. Each sample was analyzed in positive and negative modes. Conditions for the analysis in positive mode were set as described previously, with slight modification(*64*). The temperature of the LC columns was set at 40 °C. For negative mode, the chromatographic separation was performed using an ACQUITY HSS T3 column (2.1 i.d. × 50 mm, 1.8 μm; Waters, Milford, MA, USA) at 30 °C. The mobile phase, consisting of solvent A (0.1% formic acid in water) and solvent B (acetonitrile), was delivered at a flow rate of 0.3 mL/min. In this study, 50–1,200 m/z was used for the MS setting in negative mode.

Data processing from raw LC-MS data to produce a data matrix including metabolite concentration (sample × metabolite) was described previously(*65*). Data analyses were performed using MetaboAnalyst (ver. 5.0, https://www.metaboanalyst.ca/)(*65*) to produce volcano plots and to conduct pathway analysis and pattern searches. Overall data profiles were visualized using MeV TM4 (ver. 4.9.0, https://sourceforge.net/projects/mev-tm4/).

Quantification of glycine and serine enantiomers

Glycine and serine enantiomers in cell-cultured media or brain tissues were measured using two-dimensional HPLC, as previously described(*15*, *66*). Briefly, samples were mixed with 9 volumes of MeOH and centrifuged to remove protein depositions. Supernatants were spin-dried and resuspended in Milli-Q water. Resuspensions were resuspended in 200 mM sodium borate, and then derivatized with 4-fluoro-7-nitro-2,1,3-benzoxadiazole (NBD-F). NBD-conjugated amino acids were injected into a two-dimensional HPLC system (NANOSPACE SI-2 series, Shiseido, Tokyo, Japan), separated on an octadecylsilyl column (Singularity RP18, 1.0 mm inner diameter (ID) × 250 mm) (designed by Kyushu University and KAGAMI Co. Ltd., Osaka, Japan), and further separated into enantiomers on a Pirkle-type enantioselective column (Singularity CSP-001S, 1.5 mm ID × 250 mm) (designed by Kyushu University and KAGAMI). Fluorescence of NBD-amino acids was detected at 530 nm with excitation at 470 nm.

SHMT2 activity assays

The SHMT2 gene was cloned from cDNA of HeLa cells using primers 5'-GCCCATATGGCCATTCGGGCTCAGCAC-3' (forward) and 5'-GCCCTCGAGATGCTCATCAAAACCAGGCA-3' (reverse) and subcloned into the pET41a vector (Novagen, WI, USA) at restriction enzyme sites of NdeI and XhoI. C-terminally hexahistidine (His_6)-tagged human SHMT2 was purified as follows. *E. coli* BL21 (DE3) pLysS-competent cells were transformed with pET41-SHMT2, cultured at 37 °C in Luria-Bertani medium containing 20 μg/mL kanamycin, and grown until the OD600 reached 0.6-0.7. Isopropyl β-D-thiogalactopyranoside was added to a final concentration of 0.5 mM, and culturing was continued for an additional 24 h at 20°C. Harvested cells were resuspended in 20 mM sodium phosphate buffer (pH7.4) containing 500 mM NaCl and protease inhibitors (Nacalai Tesque, Kyoto, Japan), and sonicated using a Sonifier 250 instrument (Branson, CT, USA). Lysed cells were centrifuged at 20,000 × g for 10 min at 4 °C, and imidazole was added to the supernatant to a final concentration of 100 mM. The supernatant was applied to a His SpinTrap column (Cytiva, Tokyo, Japan). The column was washed with 20 mM sodium phosphate buffer (pH7.4) containing 500 mM NaCl and 100 mM imidazole. and recombinant protein was eluted with 20 mM sodium phosphate buffer (pH7.4) containing 500 mM NaCl and 500 mM imidazole. Protein fractions were buffer-exchanged into 50 mM Tris-HCl (pH8.0) containing 100 mM NaCl and 10% glycerol using an Amicon Ultra-0.5 centrifugal filter 10K device (Merck Millipore, Darmstadt, Germany).

SHMT2 activity was determined by measuring the production of glycine. The reaction mixture (150 μL) contained 50 mM HEPES-NaOH (pH8.0), 0.2 mM L-serine, 50 μM PLP, 50 μM THF, 1 mM dithiothreitol, and recombinant SHMT2 (2 μg). D-serine was added at concentrations varying from 0.1 to

0.4 mM. The reaction mixture was incubated at 37 °C for 10 min, and then 600 μL of MeOH were added to terminate the reaction. Glycine was derivatized with ortho-phthaldialdehyde (OPA) and *N*-tert-butyloxycarbonyl-L-cysteine (Boc-L-Cys), and an aliquot (10 μL) was injected into an LC-4000 Series HPLC system (Jasco Corp., Tokyo, Japan) equipped with a Mightysil RP-18GP column (150 × 4.6 mm i.d.; Kanto Chemical Co., Tokyo, Japan). A gradient of solvent A (50 mM sodium acetate buffer, pH 6.0) and solvent B (acetonitrile) was applied at a flow rate of 1 mL/min. A linear gradient was applied for 35 min from 10% to 21% solvent B for glycine analysis. Excitation and emission wavelengths for fluorescence detection were 344 nm and 443 nm, respectively.

L-serine transport assay in semi-permeabilized cells

Neuro2A cells were seeded on poly-D-lysine coated 24-well-plate, cultured for 3 days, and subjected to the transport assay. Transport of L-[^{3}H]serine was examined in semi-permeabilized cells. For plasma membrane permeabilization, cells were treated with saponin, an agent that permeabilizes the plasma membrane but leaves membranous organelles intact(*67*, *68*). The optimized saponin concentration and treatment time were verified by optical microscopy. Transport assays were performed as described previously(*69*, *70*) with some modifications. After washing the cells with 37°C pre-warmed Dulbecco's Phosphate Buffered Saline (DPBS) with 1 mM $MgCl_2$ and 0.25 mM $CaCl_2$, they were incubated for 6 min in the same buffer containing 40 μg/mL saponin (Fujifilm) for plasma membrane permeabilization. Transport of 10 μM L-[^{3}H]serine (100 Ci/mol; Moravek Biochemicals, Brea, CA, USA) with or without D-serine (at indicated concentrations) was measured for 10 min in the same buffer including saponin. After terminating the reaction and cell lysis, an aliquot of the lysate was used to measure protein concentration by BCA protein assay (Takara Bio). The lysate was mixed with OptiPhase HiSafe 3 (PerkinElmer), and radioisotope activity was monitored by LSC-8000 β-scintillation (Hitachi, Tokyo, Japan). Data shown in the figures were those subtracted from uptake values at 0 min. Kinetics of inhibition was fitted to the Nonlinear Regression: dose-response – inhibition model of GraphPad Prism 8.4.

RNA-sequence and analysis

Neuro2a cells were cultured in D-MEM with 10% FBS. The medium was changed to D-MEM(-SG) including 10% dialyzed FBS with or without 5 mM D-serine. Cells were harvested in Trizol after 18 h of incubation at 37 °C in a CO_2 incubator. RNA was extracted from cells according to the manufacture's protocol. mRNA libraries of each sample were prepared using a TruSeq Stranded mRNA library Kit (Illumina, San Diego, CA) according to the manufacturer's protocol and paired end sequences were read by NovaSeq (Illumina). Adapter sequences were trimmed from raw sequences with Trim Galore (https://www.bioinformatics.babraham.ac.uk/projects/trim_galore/) and trimmed sequences were mapped to the mouse genome (GRCm38/mm10) using HISAT2 (https://daehwankimlab.github.io/hisat2/). Aligned sequences were counted using FeatureCounts (https://subread.sourceforge.net/). Differentially expressed genes were identified by DESeq2 (https://bioconductor.org/packages/release/bioc/html/DESeq2.html). Gene Set Enrichment analysis was performed to find enriched biological pathways using ClusterProfiler (https://bioconductor.org/packages/release/bioc/html/clusterProfiler.html) with the following settings: pAdjustMethod = fd, pvalueCutoff = 0.05, minGSSize = 10, maxGSSize = 400.

Glioma stem cell culture

hG008 and hG020 cells, established from human glioblastoma specimens(*71*), were cultured in Ultra-Low attachment cell culture flasks (Corning, Kennebunk, ME, USA) in a medium, in which ingredients were manually mixed in MEM to make DMEM/Ham's F-12 with HEPES without serine and glycine (D/H-SG). The D/H-SG medium was supplemented with 2% B-27 (ThermoFisher), 20 ng/mL recombinant human fibroblast growth factor-basic (PeproTech, Rocky Hill, NJ, USA), 20 ng/mL recombinant human epidermal growth factor (PeproTech), 1000 units/mL recombinant human leukemia inhibitory factor

(Nacalai Tesque, Kyoto, Japan), and 1 unit/mL heparin. Sphere formation of hG008 cells (1×10^4 cells/well in 96-well plates with ultra-low attachment surface, Corning) was observed using EVOS M5000 (ThemoFisher) and the maximum diameter of spheres in each well was measured after 7 days of culture.

Ex vivo cancer growth assay

U87 and hG008 cells were transduced with the lentiviral vector CSII-EF-ffLuc, and single-cell suspensions were cultured in 96-well plates. Xenografts were implanted in the brain of female BALB/c nude mice as described previously[25]. Briefly, mice were implanted with Venus fluorescence-labeled U87 (5×10^5 cells/2 μL in PBS) or hG008 (1×10^5 cells/2 μL in PBS) under anesthesia on a stereotaxic apparatus (Narishige Scientific Instrument Lab, Tokyo, Japan). Mice were sacrificed after 6 days (U87) or 35 days (hG008) of implantation. Mouse brains were dissected, cut into a 200-μm slices, and cultured on the Millicell cell culture inserts (Millipore-Sigma, Burlington, MA) placed on a 35 mm glass-bottom dish filled with D/H-SG medium with or without 100 mM D-serine. Fluorescence images were taken with a FV3000 (Olympus, Tokyo, Japan) on days 0 and 7 and analyzed with Image J software (https://imagej.nih.gov/ij/index.html).

Statistics

No statistical methods were used to predetermine sample size. Blinding was not performed. No randomization was used. Prism 10 (GraphPad Software) was used for data plotting and statistical analyses. Statistical significance was determined with unpaired t-tests to compare two groups, or one-way analysis of variance (ANOVA) for multiple comparisons when data were normally distributed and had equal variance. ANOVA was followed by Dunnett's post-hoc test (comparison to control) or Tukey's post-hoc test (comparisons among samples).

Data Availability

RNA-seq data are available at Gene Expression Omnibus (GEO) with accession number GSE268106.

Acknowledgements

We thank Kenji Hamase and Masashi Mita for technical support on chiral amino acid analysis and Steven D Aird for editing the manuscript. This study was supported by the Grants-in-Aid for Scientific Research (KAKENHI) 15K19497 (MS), 17J10213 (MS), 22K19408 (JS), Keio Gijuku Fukuzawa Memorial Fund for the Advancement of Education and Research (JS), and Keio Program for the Promotion of Next Generation Research Projects Type A (JS).

Figures

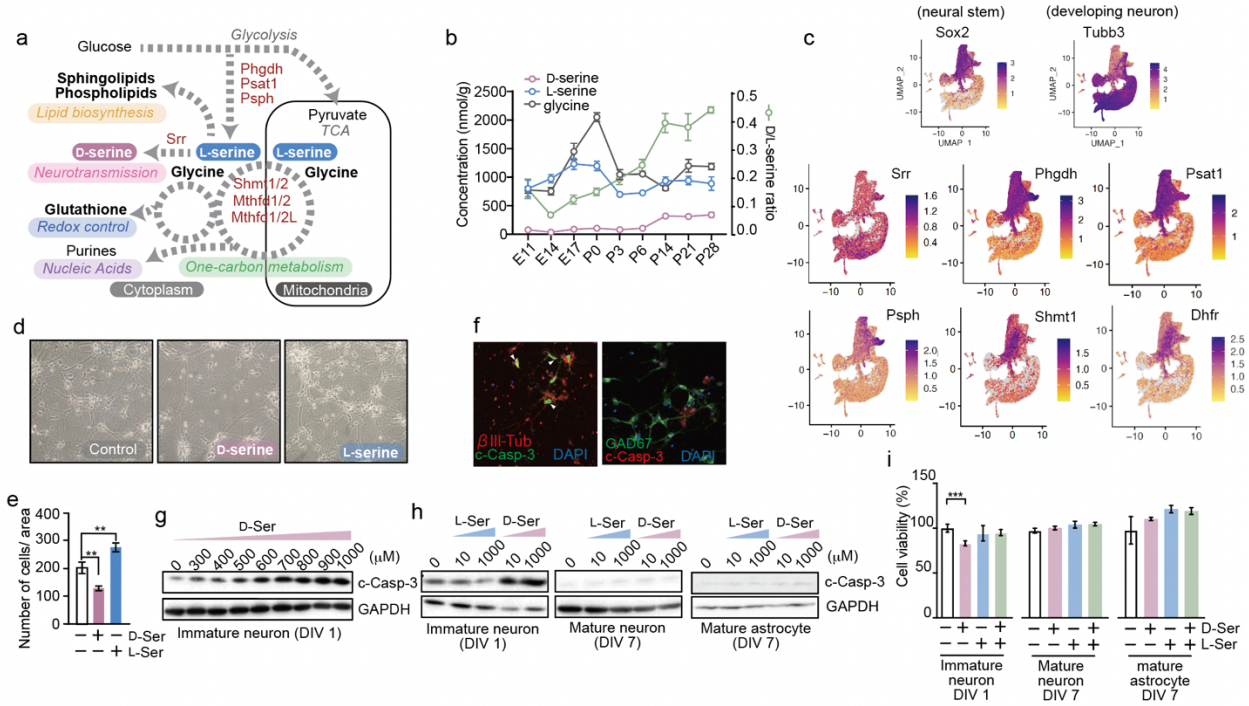

Fig. 1 Developmental transition of serine enantiomer synthesis and enantio-selective effects on immature and mature neurons

a. Metabolic flow of serine enantiomers in mammalian cells. **b**. Concentrations of serine enantiomers and glycine and the ratio of serine enantiomer concentrations in the cerebrum during development (n= 3-4). **c**. Single-cell transcriptome profiles of enzymes involved in serine metabolic pathways during mouse brain development. Original data were from Bella et al(*14*). **d**. Light microscopic view showing primary cultured NPCs treated with D- or L-serine for 7 days. **e**. Numbers of NPCs per area at DIV7 in (**d**) were counted (n = 4). **f**. Immunofluorescent images are NPCs treated with D-serine for 48 hours. Cleaved caspase-3 (c-Casp-3), green (left) or red (right); βIII Tubulin, red (left); GAD67, green (right); and DAPI (blue). **g, h**. Western blots indicate cleavage of caspase-3 in NPCs at 48 h after treatment of serine enantiomers with indicated doses starting at DIV1 (immature) or DIV7 (mature neurons or astrocytes) (n = 4). **i**. Cell viability of NPCs after 48 h treatment of serine enantiomers was analyzed. Data are plotted as the mean ± s.e.m. Statistical significance was evaluated by one-way ANOVA followed by Dunnett's post hoc test (**e** and **i**).

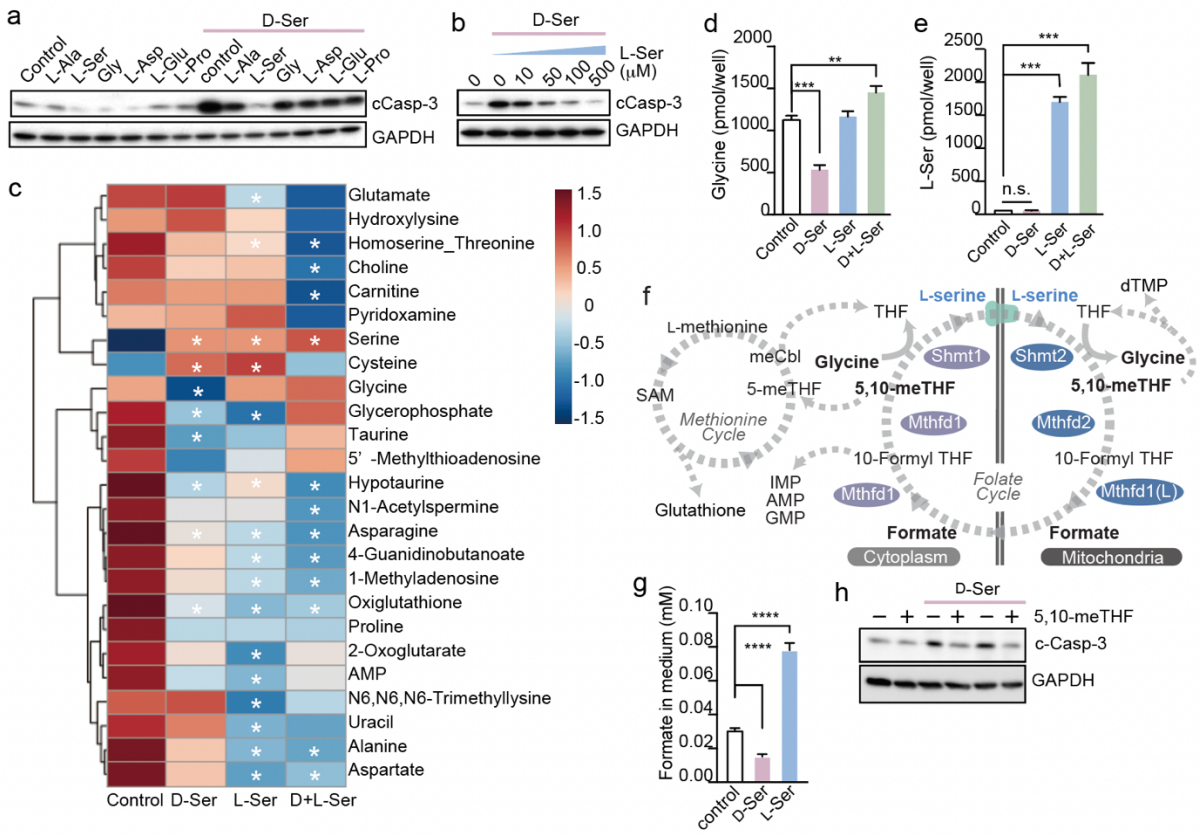

Fig. 2 D-serine toxicity mediates inhibition of one-carbon metabolism

a, b. Cleavage of caspase-3 in NPCs induced by D-serine was observed in the presence of various L-amino acids (**a**) or L-serine at indicated doses (**b**). **c**. A heatmap shows top 25 metabolites in NPCs altered by treatment with D- and/or L-serine in the metabolomic analysis (n = 3). **d, e**. Concentrations of glycine (**d**) and L-serine (**e**) in NPCs were quantified using HPLC (n = 4). **f**. Major metabolites in the one-carbon metabolism. **g.** Concentrations of formate in the culture media of NPCs treated with D- or L-serine (n = 4). **h**. Cleavage of caspase-3 in NPCs triggered by D-serine was observed in the presence or absence of 5,10-meTHF. Data are presented as the mean ± s.e.m. (**d, e,** and **g**). Statistical significance was evaluated by one-way ANOVA followed by Dunnett's post hoc-test (**c, d, e,** and **g**). *$p < 0.05$ (**c**).

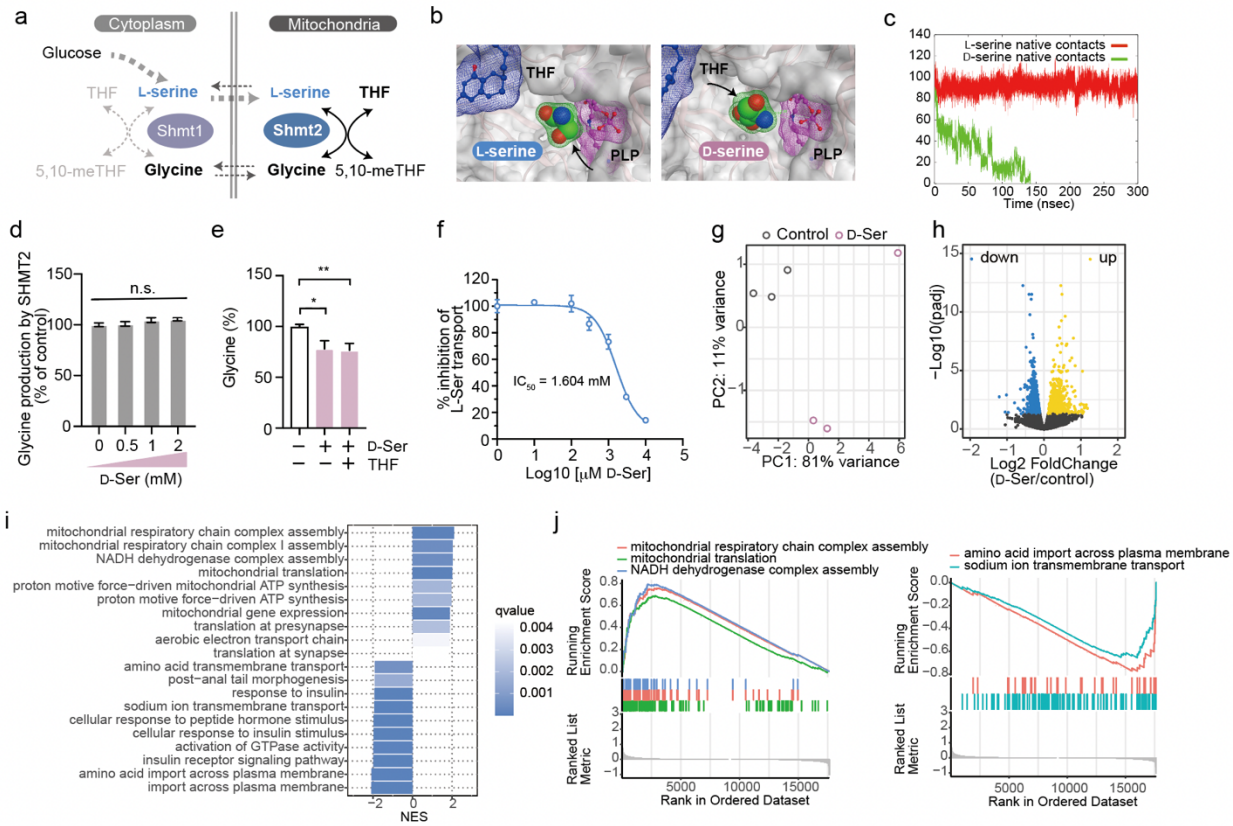

Fig. 3 D-serine inhibits cytoplasmic L-serine transport to mitochondria

a. L-serine/glycine transport and conversion across cytoplasm and mitochondria in one-carbon metabolism. **b.** Binding sites of D- (right) or L-serine (left), THF, and pyridoxal phosphate (PLP) in the ligand-bound SHMT2 complex systems. Arrows indicate carbon atoms on serine enantiomers that transfer to THF. **c.** Time series variation of the number of contact atoms within the distance cutoff of 7.0 Å from D- or L-serine observed at the initial structure. **d.** SHMT2 enzymatic activity determined by glycine production is shown as percent of control (with no D-serine) (n = 3). **e.** Relative concentrations of glycine in NPCs treated with or without D-serine and/or THF. **f.** Inhibition of mitochondrial L-serine transport by D-serine was examined in semi-permeabilized cells (n = 4). **g.** A PCA plot shows RNA-seq results from cells treated with D-serine (pink) or control (gray). **h.** A volcano plot indicates differentially expressed genes in cells treated with D-serine vs controls. Gene expressions with *p*-values < 0.05 are highlighted in yellow (up) or blue (down). **i.** Bar plots show Normalized Enrichment Score for the top 10 up or down-regulated GSEA-enriched categories. Color, q-value. **j.** GSEA plots for a core subset of gene ontologies are displayed. Data are plotted as the mean ± s.e.m. (**d, e,** and **f**). Statistical significance was evaluated by one-way ANOVA followed by Tukey's post hoc-test (**d**) or Dunnett's post hoc-test (**e**).

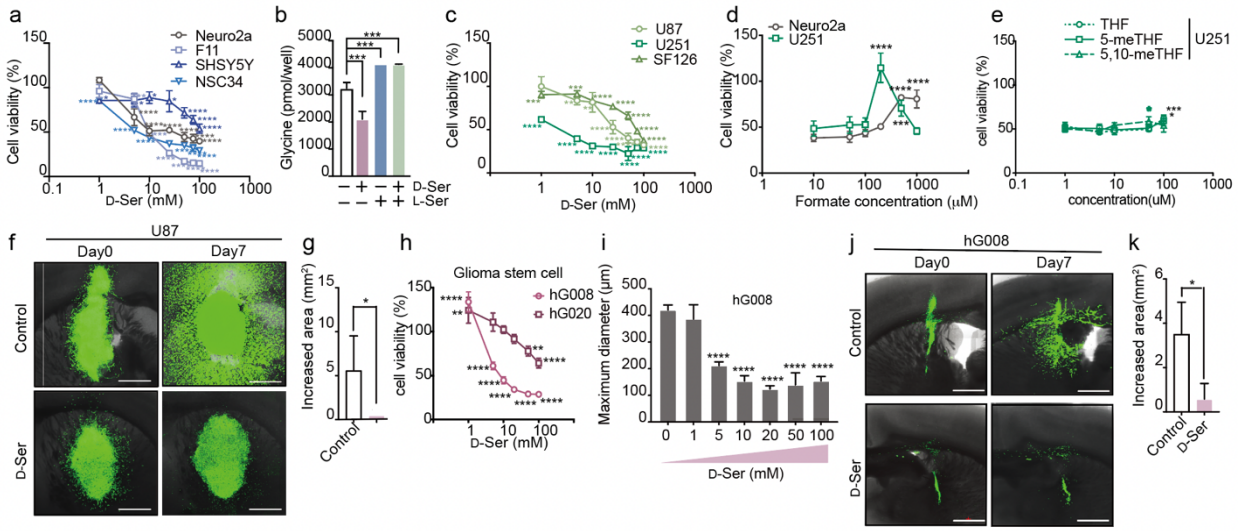

Fig. 4 D-serine attenuates proliferation of neural tumor cells

a, c, h. Viabilities of neuroblastoma cell lines (**a**), glioblastoma lines (**c**), and glioma stem cells (**h**) treated with D-serine at indicated doses were analyzed 48 h after treatment (n = 4, each). Cells with the vehicle treatment were used as 100% viability controls. **b**. Glycine concentration in Neuro2a cells was quantified 48 h after treatment with D- and/or L-serine (n = 3). **d, e**. Cell viabilities were assessed 48 h after treatment with 5mM D-serine and formate/folates at indicated doses (n = 4). Viabilities were compared to those of cells treated with D-serine alone. **f, g, j, k.** *Ex vivo* slice cultures of mouse brain transplanted with U87 (**f, g**) or hG008 cells (**j, k**) expressing Venus fluorescence were treated with D-serine. Representative images of the xenograft at 0 and 7 days after treatment are shown (**f, j**). Increased area of fluorescence after 7 days of culture was measured (**g, k**). **i**. Sphere diameters of glioma stem cells (hG008) were measured at 7 days after treatment with D-serine at indicated doses. Data are presented as the mean ± s.e.m. (**a-e, g-i,** and **k**). Statistical significance was evaluated by one-way ANOVA followed by Dunnett's post-hoc test (**b, d,** and **e**) or by Student's t-test (**g** and **k**).

References

1. S. L. Geeraerts, E. Heylen, K. D. Keersmaecker, K. R. Kampen, The ins and outs of serine and glycine metabolism in cancer. *Nat. Metab.* **3**, 131–141 (2021).

2. Y. Hirabayashi, S. Furuya, Roles of l-serine and sphingolipid synthesis in brain development and neuronal survival. *Prog. Lipid Res.* **47**, 188–203 (2008).

3. K. W. Nancy, R. Dingledine, Requirement for Glycine in Activation of NMDA-Receptors Expressed in Xenopus Oocytes. *science* (1988).

4. J. E. Chatterton, M. Awobuluyi, L. S. Premkumar, H. Takahashi, M. Talantova, Y. Shin, J. Cui, S. Tu, K. A. Sevarino, N. Nakanishi, G. Tong, S. A. Lipton, D. Zhang, Excitatory glycine receptors containing the NR3 family of NMDA receptor subunits. *Nature* **415**, 793–798 (2002).

5. J. W. Lynch, Molecular Structure and Function of the Glycine Receptor Chloride Channel. *Physiol. Rev.* **84**, 1051–1095 (2004).

6. J. Jaeken, M. Detheux, J. P. Fryns, J. F. Collet, P. Alliet, E. V. Schaftingen, Phosphoserine phosphatase deficiency in a patient with Williams syndrome. *J. Méd. Genet.* **34**, 594 (1997).

7. T. J. D. KONING, M. DURAN, L. V. MALDERGEM, M. PINEDA, L. DORLAND1, R. GOOSKENS, J. J. and B. T. POLL-T, Congenital microcephaly and seizures due to 3-phosphoglycerate dehydrogenase deficiency: Outcome of treatment with amino acids. *J. Inherit. Metab. Dis* (2002).

8. K. Yoshida, S. Furuya, S. Osuka, J. Mitoma, Y. Shinoda, M. Watanabe, N. Azuma, H. Tanaka, T. Hashikawa, S. Itohara, Y. Hirabayashi, Targeted Disruption of the Mouse 3-Phosphoglycerate Dehydrogenase Gene Causes Severe Neurodevelopmental Defects and Results in Embryonic Lethality*. *J. Biol. Chem.* **279**, 3573–3577 (2004).

9. J. H. Yang, A. Wada, K. Yoshida, Y. Miyoshi, T. Sayano, K. Esaki, M. O. Kinoshita, S. Tomonaga, N. Azuma, M. Watanabe, K. Hamase, K. Zaitsu, T. Machida, A. Messing, S. Itohara, Y. Hirabayashi, S. Furuya, Brain-specific Phgdh Deletion Reveals a Pivotal Role for l-Serine Biosynthesis in Controlling the Level of d-Serine, an N-methyl-d-aspartate Receptor Co-agonist, in Adult Brain*. *J. Biol. Chem.* **285**, 41380–41390 (2010).

10. J.-P. Mothet, A. T. Parent, H. Wolosker, R. O. Brady, D. J. Linden, C. D. Ferris, M. A. Rogawski, S. H. Snyder, d-Serine is an endogenous ligand for the glycine site of the N-methyl-d-aspartate receptor. *Proc. Natl. Acad. Sci.* **97**, 4926–4931 (2000).

11. H. Wolosker, D. T. Balu, d-Serine as the gatekeeper of NMDA receptor activity: implications for the pharmacologic management of anxiety disorders. *Transl. Psychiatry* **10**, 184 (2020).

12. K. S. Hubbard, I. M. Gut, M. E. Lyman, P. M. McNutt, Longitudinal RNA sequencing of the deep transcriptome during neurogenesis of cortical glutamatergic neurons from murine ESCs. *F1000research* **2**, 35 (2013).

13. E. E. Burke, J. G. Chenoweth, J. H. Shin, L. Collado-Torres, S.-K. Kim, N. Micali, Y. Wang, C. Colantuoni, R. E. Straub, D. J. Hoeppner, H.-Y. Chen, A. Sellers, K. Shibbani, G. R. Hamersky, M. D. Bustamante, B. N. Phan, W. S. Ulrich, C. Valencia, A. Jaishankar, A. J. Price, A. Rajpurohit, S. A. Semick, R. W. Bürli, J. C. Barrow, D. J. Hiler, S. C. Page, K. Martinowich, T. M. Hyde, J. E. Kleinman, K. F. Berman, J. A. Apud, A. J. Cross, N. J. Brandon, D. R. Weinberger, B. J. Maher, R. D. G. McKay, A. E. Jaffe, Dissecting transcriptomic signatures of neuronal differentiation and maturation using iPSCs. *Nat Commun* **11**, 462 (2020).

14. D. J. D. Bella, E. Habibi, R. R. Stickels, G. Scalia, J. Brown, P. Yadollahpour, S. M. Yang, C. Abbate, T. Biancalani, E. Z. Macosko, F. Chen, A. Regev, P. Arlotta, Molecular logic of cellular diversification in the mouse cerebral cortex. *Nature* **595**, 554–559 (2021).

15. Y. Gonda, A. Matsuda, K. Adachi, C. Ishii, M. Suzuki, A. Osaki, M. Mita, N. Nishizaki, Y. Ohtomo, T. Shimizu, M. Yasui, K. Hamase, J. Sasabe, Mammals sustain amino acid homochirality against chiral conversion by symbiotic microbes. *Proc Natl Acad Sci U S A*, doi: 10.1073/pnas.2300817120 (2023).

16. H. K. Park, Y. Shishido, S. Ichise-Shishido, T. Kawazoe, K. Ono, S. Iwana, Y. Tomita, K. Yorita, T. Sakai, K. Fukui, Potential Role for Astroglial d-Amino Acid Oxidase in Extracellular d-Serine Metabolism and Cytotoxicity. *J. Biochem.* **139**, 295–304 (2006).

17. D. McNamara, R. Dingledine, Dual effect of glycine on NMDA-induced neurotoxicity in rat cortical cultures. *J. Neurosci.* **10**, 3970–3976 (1990).

18. S. Pan, M. Fan, Z. Liu, X. Li, H. Wang, Serine, glycine and one-carbon metabolism in cancer (Review). *Int J Oncol* **58**, 158–170 (2020).

19. G. S. Ducker, L. Chen, R. J. Morscher, J. M. Ghergurovich, M. Esposito, X. Teng, Y. Kang, J. D. Rabinowitz, Reversal of Cytosolic One-Carbon Flux Compensates for Loss of the Mitochondrial Folate Pathway. *Cell Metab.* **23**, 1140–1153 (2016).

20. T. Miyamoto, S. Fushinobu, Y. Saitoh, M. Sekine, M. Katane, K. Sakai-Kato, H. Homma, Novel tetrahydrofolate-dependent d-serine dehydratase activity of serine hydroxymethyltransferases. *FEBS J.* **291**, 308–322 (2024).

21. T. Reya, S. J. Morrison, M. F. Clarke, I. L. Weissman, Stem cells, cancer, and cancer stem cells. *Nature* **414**, 105–111 (2001).

22. M. J. McNamee, D. Michod, M. V. Niklison-Chirou, Can small molecular inhibitors that stop de novo serine synthesis be used in cancer treatment? *Cell Death Discov* **7**, 87 (2021).

23. M. J. van den Bent, M. Geurts, P. J. French, M. Smits, D. Capper, J. E. C. Bromberg, S. M. Chang, Primary brain tumours in adults. *Lancet* **402**, 1564–1579 (2023).

24. P. D. Delgado-López, E. M. Corrales-García, Survival in glioblastoma: a review on the impact of treatment modalities. *Clin. Transl. Oncol.* **18**, 1062–1071 (2016).

25. R. Tamura, H. Miyoshi, O. Sampetrean, M. Shinozaki, Y. Morimoto, C. Iwasawa, R. Fukaya, Y. Mine, H. Masuda, T. Maruyama, M. Narita, H. Saya, K. Yoshida, H. Okano, M. Toda, Visualization of spatiotemporal dynamics of human glioma stem cell invasion. *Mol. Brain* **12**, 45 (2019).

26. R. C. Gimple, K. Yang, M. E. Halbert, S. Agnihotri, J. N. Rich, Brain cancer stem cells: resilience through adaptive plasticity and hierarchical heterogeneity. *Nat. Rev. Cancer* **22**, 497–514 (2022).

27. X. Tang, C. Zuo, P. Fang, G. Liu, Y. Qiu, Y. Huang, R. Tang, Targeting Glioblastoma Stem Cells: A Review on Biomarkers, Signal Pathways and Targeted Therapy. *Front. Oncol.* **11**, 701291 (2021).

28. A. Hashimoto, T. Nishikawa, T. Oka, K. Takahashi, Endogenous d-Serine in Rat Brain: N-Methyl-d-Aspartate Receptor-Related Distribution and Aging. *J. Neurochem.* **60**, 783–786 (1993).

29. K. Miya, R. Inoue, Y. Takata, M. Abe, R. Natsume, K. Sakimura, K. Hongou, T. Miyawaki, H. Mori, Serine racemase is predominantly localized in neurons in mouse brain. *J. Comp. Neurol.* **510**, 641–654 (2008).

30. D. T. Balu, S. Takagi, M. D. Puhl, M. A. Benneyworth, J. T. Coyle, d-Serine and Serine Racemase are Localized to Neurons in the Adult Mouse and Human Forebrain. *Cell. Mol. Neurobiol.* **34**, 419–435 (2014).

31. A. C. Basu, G. E. Tsai, C.-L. Ma, J. T. Ehmsen, A. K. Mustafa, L. Han, Z. I. Jiang, M. A. Benneyworth, M. P. Froimowitz, N. Lange, S. H. Snyder, R. Bergeron, J. T. Coyle, Targeted disruption of serine racemase affects glutamatergic neurotransmission and behavior. *Mol. Psychiatry* **14**, 719–727 (2009).

32. D. T. Balu, A. C. Basu, J. P. Corradi, A. M. Cacace, J. T. Coyle, The NMDA receptor co-agonists, d-serine and glycine, regulate neuronal dendritic architecture in the somatosensory cortex. *Neurobiol. Dis.* **45**, 671–682 (2012).

33. M. R. V. Horn, A. Strasser, L. S. Miraucourt, L. Pollegioni, E. S. Ruthazer, The Gliotransmitter d-Serine Promotes Synapse Maturation and Axonal Stabilization In Vivo. *J. Neurosci.* **37**, 6277–6288 (2017).

34. S. Sultan, L. Li, J. Moss, F. Petrelli, F. Cassé, E. Gebara, J. Lopatar, F. W. Pfrieger, P. Bezzi, J. Bischofberger, N. Toni, Synaptic Integration of Adult-Born Hippocampal Neurons Is Locally Controlled by Astrocytes. *Neuron* **88**, 957–972 (2015).

35. J. Nomura, H. Jaaro-Peled, E. Lewis, P. Nuñez-Abades, F. Huppe-Gourgues, T. Cash-Padgett, F. Emiliani, M. A. Kondo, A. Furuya, M. A. Landek-Salgado, Y. Ayhan, A. Kamiya, T. Takumi, R. Huganir, M. Pletnikov, P. O'Donnell, A. Sawa, Role for neonatal D-serine signaling: prevention of physiological and behavioral deficits in adult Pick1 knockout mice. *Mol. Psychiatry* **21**, 386–393 (2016).

36. M. Shleper, E. Kartvelishvily, H. Wolosker, D-Serine Is the Dominant Endogenous Coagonist for NMDA Receptor Neurotoxicity in Organotypic Hippocampal Slices. *J Neurosci* **25**, 9413–9417 (2005).

37. J. Patel, W. C. Zinkand, C. Thompson, R. Keith, A. Salama, Role of Glycine in the N-Methyl-d-Aspartate-Mediated Neuronal Cytotoxicity. *J. Neurochem.* **54**, 849–854 (1990).

38. J. P. Kaltenbach, C. E. Ganote, F. A. Carone, Renal tubular necrosis induced by compounds structurally related to d-serine. *Exp. Mol. Pathol.* **30**, 209–214 (1979).

39. R. E. Williams, E. A. Lock, d-Serine-induced nephrotoxicity: possible interaction with tyrosine metabolism. *Toxicology* **201**, 231–238 (2004).

40. J. Sasabe, T. Chiba, M. Yamada, K. Okamoto, I. Nishimoto, M. Matsuoka, S. Aiso, D-Serine is a key determinant of glutamate toxicity in amyotrophic lateral sclerosis. *EMBO J.* **26**, 4149–4159 (2007).

41. A. K. Mustafa, A. S. Ahmad, E. Zeynalov, S. K. Gazi, G. Sikka, J. T. Ehmsen, R. K. Barrow, J. T. Coyle, S. H. Snyder, S. Doré, Serine Racemase Deletion Protects Against Cerebral Ischemia and Excitotoxicity. *J. Neurosci.* **30**, 1413–1416 (2010).

42. R. Inoue, K. Hashimoto, T. Harai, H. Mori, NMDA- and β-Amyloid1–42-Induced Neurotoxicity Is Attenuated in Serine Racemase Knock-Out Mice. *J. Neurosci.* **28**, 14486–14491 (2008).

43. M. Maekawa, T. Okamura, N. Kasai, Y. Hori, K. H. Summer, R. Konno, d-Amino-acid Oxidase Is Involved in d-Serine-Induced Nephrotoxicity. *Chem. Res. Toxicol.* **18**, 1678–1682 (2005).

44. Y. Gonda, C. Ishii, M. Mita, N. Nishizaki, Y. Ohtomo, K. Hamase, T. Shimizu, J. Sasabe, Astrocytic d-amino acid oxidase degrades d-serine in the hindbrain. *FEBS Lett.* **596**, 2889–2897 (2022).

45. A. Okada, M. Nangaku, T.-M. Jao, H. Maekawa, Y. Ishimono, T. Kawakami, R. Inagi, D-serine, a novel uremic toxin, induces senescence in human renal tubular cells via GCN2 activation. *Sci. Rep.* **7**, 11168 (2017).

46. G. S. Ducker, J. D. Rabinowitz, One-Carbon Metabolism in Health and Disease. *Cell Metab* **25**, 27–42 (2017).

47. R. Acuna-Hidalgo, D. Schanze, A. Kariminejad, A. Nordgren, M. H. Kariminejad, P. Conner, G. Grigelioniene, D. Nilsson, M. Nordenskjöld, A. Wedell, C. Freyer, A. Wredenberg, D. Wieczorek, G. Gillessen-Kaesbach, H. Kayserili, N. Elcioglu, S. Ghaderi-Sohi, P. Goodarzi, H. Setayesh, M. van de Vorst, M. Steehouwer, R. Pfundt, B. Krabichler, C. Curry, M. G. MacKenzie, K. M. Boycott, C. Gilissen, A. R. Janecke, A. Hoischen, M. Zenker, Neu-Laxova Syndrome Is a Heterogeneous Metabolic Disorder Caused by Defects in Enzymes of the L-Serine Biosynthesis Pathway. *Am. J. Hum. Genet.* **95**, 285–293 (2014).

48. A. E. Beaudin, P. J. Stover, Insights into metabolic mechanisms underlying folate-responsive neural tube defects: A minireview. *Birth Defects Res. Part A: Clin. Mol. Teratol.* **85**, 274–284 (2009).

49. A. J. MacFarlane, X. Liu, C. A. Perry, P. Flodby, R. H. Allen, S. P. Stabler, P. J. Stover, Cytoplasmic Serine Hydroxymethyltransferase Regulates the Metabolic Partitioning of Methylenetetrahydrofolate but Is Not Essential in Mice*. *J. Biol. Chem.* **283**, 25846–25853 (2008).

50. N. Kory, G. A. Wyant, G. Prakash, J. uit de Bos, F. Bottanelli, M. E. Pacold, S. H. Chan, C. A. Lewis, T. Wang, H. R. Keys, Y. E. Guo, D. M. Sabatini, SFXN1 is a mitochondrial serine transporter required for one-carbon metabolism. *Science* **362** (2018).

51. C. F. Labuschagne, N. J. F. van den Broek, G. M. Mackay, K. H. Vousden, O. D. K. Maddocks, Serine, but Not Glycine, Supports One-Carbon Metabolism and Proliferation of Cancer Cells. *Cell Reports* **7**, 1248–1258 (2014).

52. M. Jain, R. Nilsson, S. Sharma, N. Madhusudhan, T. Kitami, A. L. Souza, R. Kafri, M. W. Kirschner, C. B. Clish, V. K. Mootha, Metabolite profiling identifies a key role for glycine in rapid cancer cell proliferation. *Science* **336**, 1037–1040 (2012).

53. G. Y. Lee, P. M. Haverty, L. Li, N. M. Kljavin, R. Bourgon, J. Lee, H. Stern, Z. Modrusan, S. Seshagiri, Z. Zhang, D. Davis, D. Stokoe, J. Settleman, F. J. de Sauvage, R. M. Neve, Comparative Oncogenomics Identifies PSMB4 and SHMT2 as Potential Cancer Driver Genes. *Cancer Res.* **74**, 3114–3126 (2014).

54. C. A. Lewis, S. J. Parker, B. P. Fiske, D. McCloskey, D. Y. Gui, C. R. Green, N. I. Vokes, A. M. Feist, M. G. Vander Heiden, C. M. Metallo, Tracing Compartmentalized NADPH Metabolism in the Cytosol and Mitochondria of Mammalian Cells. *Mol. Cell* **55**, 253–263 (2014).

55. R. Nilsson, M. Jain, N. Madhusudhan, N. G. Sheppard, L. Strittmatter, C. Kampf, J. Huang, A. Asplund, V. K. Mootha, Metabolic enzyme expression highlights a key role for MTHFD2 and the mitochondrial folate pathway in cancer. *Nat. Commun.* **5**, 3128 (2014).

56. A. C. Newman, O. D. K. Maddocks, One-carbon metabolism in cancer. *Br. J. Cancer* **116**, 1499–1504 (2017).

57. Y. Miyoshi, K. Hamase, Y. Tojo, M. Mita, R. Konno, K. Zaitsu, Determination of d-serine and d-alanine in the tissues and physiological fluids of mice with various d-amino-acid oxidase activities using two-dimensional high-performance liquid chromatography with fluorescence detection. *J. Chromatogr. B* **877**, 2506–2512 (2009).

58. Y. Nagata, K. Horiike, T. Maeda, Distribution of freed-serine in vertebrate brains. *Brain Res* **634**, 291–295 (1994).

59. H. Furukawa, E. Gouaux, Mechanisms of activation, inhibition and specificity: crystal structures of the NMDA receptor NR1 ligand-binding core. *The EMBO Journal*, doi: 10.1093/emboj/cdg303 (2003).

60. J. M. Archibald, Endosymbiosis and Eukaryotic Cell Evolution. *Curr. Biol.* **25**, R911–R921 (2015).

61. S. D. Cosloy, E. McFall, Metabolism of d-Serine in Escherichia coli K-12: Mechanism of Growth Inhibition. *J. Bacteriol.* **114**, 685–694 (1973).

62. M. Tajan, M. Hennequart, E. C. Cheung, F. Zani, A. K. Hock, N. Legrave, O. D. K. Maddocks, R. A. Ridgway, D. Athineos, A. Suárez-Bonnet, R. L. Ludwig, L. Novellasdemunt, N. Angelis, V. S. W. Li, G. Vlachogiannis, N. Valeri, N. Mainolfi, V. Suri, A. Friedman, M. Manfredi, K. Blyth, O. J. Sansom, K. H. Vousden, Serine synthesis pathway inhibition cooperates with dietary serine and glycine limitation for cancer therapy. *Nat Commun* **12**, 366 (2021).

63. S. Fuse, M. Sugimoto, Y. Kurosawa, M. Kuroiwa, Y. Aita, A. Tomita, E. Yamaguchi, R. Tanaka, T. Endo, R. Kime, T. Hamaoka, Relationships between plasma lipidomic profiles and brown adipose tissue density in humans. *Int. J. Obes.* **44**, 1387–1396 (2020).

64. A. Tomita, M. Mori, K. Hiwatari, E. Yamaguchi, T. Itoi, M. Sunamura, T. Soga, M. Tomita, M. Sugimoto, Effect of storage conditions on salivary polyamines quantified via liquid chromatography-mass spectrometry. *Sci. Rep.* **8**, 12075 (2018).

65. Z. Pang, J. Chong, G. Zhou, D. A. de Lima Morais, L. Chang, M. Barrette, C. Gauthier, P.-É. Jacques, S. Li, J. Xia, MetaboAnalyst 5.0: narrowing the gap between raw spectra and functional insights. *Nucleic Acids Res.* **49**, gkab382- (2021).

66. C. Ishii, T. Akita, M. Mita, T. Ide, K. Hamase, Development of an online two-dimensional high-performance liquid chromatographic system in combination with tandem mass spectrometric detection for enantiomeric analysis of free amino acids in human physiological fluid. *J. Chromatogr. A* **1570**, 91–98 (2018).

67. A. Klepinin, L. Ounpuu, R. Guzun, V. Chekulayev, N. Timohhina, K. Tepp, I. Shevchuk, U. Schlattner, T. Kaambre, Simple oxygraphic analysis for the presence of adenylate kinase 1 and 2 in normal and tumor cells. *J. Bioenerg. Biomembr.* **48**, 531–548 (2016).

68. A. V. Kuznetsov, V. Veksler, F. N. Gellerich, V. Saks, R. Margreiter, W. S. Kunz, Analysis of mitochondrial function in situ in permeabilized muscle fibers, tissues and cells. *Nat. Protoc.* **3**, 965–976 (2008).

69. Y. Lee, P. Wiriyasermkul, P. Kongpracha, S. Moriyama, D. J. Mills, W. Kühlbrandt, S. Nagamori, Ca2+-mediated higher-order assembly of heterodimers in amino acid transport system b0,+ biogenesis and cystinuria. *Nat. Commun.* **13**, 2708 (2022).

70. P. Wiriyasermkul, S. Nagamori, H. Tominaga, N. Oriuchi, K. Kaira, H. Nakao, T. Kitashoji, R. Ohgaki, H. Tanaka, H. Endou, K. Endo, H. Sakurai, Y. Kanai, Transport of 3-Fluoro-l-α-Methyl-Tyrosine by Tumor-Upregulated L-Type Amino Acid Transporter 1: A Cause of the Tumor Uptake in PET. *J. Nucl. Med.* **53**, 1253–1261 (2012).

71. R. Fukaya, S. Ohta, T. Yaguchi, Y. Matsuzaki, E. Sugihara, H. Okano, H. Saya, Y. Kawakami, T. Kawase, K. Yoshida, M. Toda, MIF Maintains the Tumorigenic Capacity of Brain Tumor–Initiating Cells by Directly Inhibiting p53. *Cancer Res.* **76**, 2813–2823 (2016).